



# APPLICATION OF A PHASE AND AMPLITUDE GRADIENT ESTIMATOR TO INTENSITY-BASED LABORATORY-SCALE JET NOISE SOURCE CHARACTERIZATION

Kent L. Gee<sup>1</sup>, Tracianne B. Neilsen<sup>1</sup>, Eric B. Whiting<sup>1</sup>, Darren K. Torrie<sup>1</sup>, Masahito Akamine<sup>2</sup>, Koji Okamoto<sup>2</sup>, Susumu Teramoto<sup>3</sup>, and Seiji Tsutsumi<sup>4</sup>

<sup>1</sup>Department of Physics and Astronomy, Brigham Young University  
Provo, UT 84602, USA

<sup>2</sup>Graduate School of Frontier Sciences, University of Tokyo  
Kashiwa, Chiba, 277-8561, Japan

<sup>3</sup>Graduate School of Engineering, University of Tokyo  
Bunkyo-ku, Tokyo, 113-8656, Japan

<sup>4</sup>Japan Aerospace Exploration Agency, Sagami-hara, Kanagawa, 252-5210, Japan

## ABSTRACT

A new method for the calculation of vector acoustic intensity from pressure microphone measurements has been applied to the aeroacoustic source characterization of an unheated, Mach 1.8 laboratory-scale jet. Because of the ability to unwrap the phase of the transfer functions between microphone pairs in the measurement of a broadband source, physically meaningful near-field intensity vectors are calculated up to the maximum analysis frequency of 32 kHz. This result improves upon the bandwidth of the traditional cross-spectral intensity calculation method by nearly an order of magnitude. The new intensity method is used to obtain a detailed description of the sound energy flow near the jet. The resulting intensity vectors have been used in a ray-tracing technique to identify the dominant source region over a broad range of frequencies. Additional aeroacoustics analyses provide insight into the frequency-dependent characteristics of jet noise radiation, including the nature of the hydrodynamic field and the sharp transition between the Mach wave and sideline radiation.

## 1 INTRODUCTION

Vector acoustic intensity, which can be used to describe the flow of sound energy around and from a radiating source, is an important industry tool within acoustical engineering. In addition to standardized methods [1-3] for obtaining radiated power from a source, intensity has been applied to, e.g., noise source identification [4] and in characterizing building insulation [5].

Despite acoustic intensity's use as robust engineering tool, the technique has not been heavily utilized to characterize the source region of turbulent jet flows. Jaeger and Allen [6] performed bandlimited, two-dimensional vector intensity measurements of a Mach 0.2-0.6

laboratory-scale, unheated jet. The authors traced intensity vectors directly back to the jet centerline, using the intercepts to describe the source region. As expected from the low Mach number, the intensity vectors were found to originate from a relatively compact region. In addition to the study by Jaeger and Allen, Ventakesh *et al.* [7] briefly described the use of a one-dimensional intensity probe to validate the results of a new beamforming algorithm for distributed, broadband sources. Recently, efforts have been made to characterize rocket plume environments using vector acoustic intensity [8-10]. These efforts also motivated parallel studies of the noise source region for the F-22A Raptor at both military thrust and afterburner [11,12]. In conjunction with the rocket plume measurement developments, a new method [13] for calculating vector intensity was developed that extends the useable bandwidth of the measurement probes.

The present study describes the application of the recently developed phase and amplitude gradient estimator (PAGE) method [13] for calculating vector acoustic intensity to the wideband near-field characterization of a laboratory-scale supersonic jet. The PAGE method is first summarized, followed by a description of the experimental facilities and measurement performed. The traditional and PAGE methods are compared in their abilities to obtain physically reasonable results, and the PAGE method is used to characterize the jet noise source. The results indicate an approximate order-of-magnitude extension of the upper frequency bandwidth of the intensity probe using the PAGE method and point to the potential of the method to dramatically improve characterization of supersonic jet noise sources.

## 2 SUMMARY OF ACOUSTIC INTENSITY AND THE PAGE METHOD

The time-averaged vector acoustic intensity stems from the product of the time-dependent pressure and vector particle velocity,

$$\mathbf{I} = \frac{1}{T} \int p(t) \mathbf{u}(t) dt, \quad (1)$$

where the bold-faced notation indicates a vector. From two well matched microphones, Fahy [14] and Pavic [15] determined a means to calculate the frequency-domain intensity spectrum, still the standardized approach used today. The time-averaged acoustic intensity component along the  $x$  axis for two microphones spaced  $\Delta x$  apart is written as

$$I_x(\omega) = \frac{1}{\rho_0 \omega \Delta x} Q_{2,1}(\omega), \quad (2)$$

where  $\rho_0$  is the ambient density and  $Q_{2,1}(\omega)$  is the imaginary part of the cross spectrum (the quadspectrum) between the two microphones. From the single-axis intensity probes, many have developed multidimensional acoustic intensity probes. For these probes involving multiple combinations of microphone pairs, the optimal intensity calculations are obtained using least-squares weighting of quadspectra, as described by Pascal and Li [16] and Wiederhold *et al.* [17,18]. The bias errors associated with the traditional method have generally resulted in substantial bandwidth limitations. For example, intensity magnitude errors for two well-matched microphones separated by 25 mm in a propagating plane wave field exceed 1 dB beginning at about 2.5 kHz.

The PAGE method [13] improves on the traditional cross-spectral approach by estimating gradients of the pressure phase and amplitude across a multimicrophone probe to calculate the complex intensity. The methodology builds from the work of Mann [19-21] and colleagues, who theoretically interpreted the radiated intensity and other energy-based quantities. As part of their work, they expressed the spatially dependent complex pressure at position,  $\mathbf{r}$ , in terms of a pressure magnitude and phase,  $p(\mathbf{r}) = P(\mathbf{r})e^{-j\phi(\mathbf{r})}$ . By Euler's equation for a time-harmonic acoustic process, the particle velocity is calculated in terms of  $\nabla p$  as

$$\mathbf{u}(\mathbf{r}) = \frac{j}{\rho_0\omega} \nabla p = \frac{1}{\rho_0\omega} [P(\mathbf{r})\nabla\phi(\mathbf{r}) + j\nabla P(\mathbf{r})]e^{-j\phi(\mathbf{r})}, \quad (3)$$

which, from Eq. (1), results in an expression for the radiated (active) intensity as

$$\mathbf{I} = \frac{1}{2\rho_0\omega} P^2 \nabla\phi = \frac{1}{\rho_0\omega} \overline{P^2} \nabla\phi, \quad (4)$$

where  $\overline{P^2}$  is the mean-square pressure. Although Mann *et al.* [19] considered this alternate expression theoretically, it is noteworthy that Mann and Tichy [21] stepped from this expression directly to the traditional cross-spectral approach when describing actual measurements.

In the PAGE method,  $\overline{P^2}$  can be readily found by locating a microphone at the acoustic center of the probe or, alternatively, by finding a least-squares estimate of the pressure magnitude [17,18]. (For the probe geometry used in the experiments, a microphone was located at the probe center.) The phase gradient,  $\nabla\phi$ , is calculated for  $N$  microphones located at positions,  $\mathbf{r}_{1..N}$ , by first defining a position difference vector,  $\mathbf{X}$ , written as

$$\mathbf{X} = [\mathbf{r}_2 - \mathbf{r}_1 \mid \dots \mid \mathbf{r}_N - \mathbf{r}_{N-1}]^T \quad (5)$$

and then finding the least-squares estimate for the gradient, expressed as

$$\nabla\phi \approx (\mathbf{X}^T \mathbf{X})^{-1} \mathbf{X}^T \Delta\phi. \quad (6)$$

The ensemble-averaged phase difference between microphones,  $\Delta\phi$ , in Eq. (4) can be found through the argument of the transfer function between different microphone pairs, written as

$$\Delta\phi = -[\arg\{H_{1,2}\} \mid \dots \mid \arg\{H_{N-1,N}\}]^T. \quad (7)$$

Note that whereas the traditional cross-spectral method is limited to well below the spatial Nyquist limit because of the calculation bias errors, the use of the transfer function phase in the PAGE method allows for the direct possibility of phase unwrapping for a broadband source. [13] As demonstrated in Sec. 4.2 and beyond, phase unwrapping can significantly extend the frequency bandwidth of the PAGE method, well beyond the traditional high-frequency limit.

### 3 EXPERIMENT

#### 3.1 Jet Facility

The experiment was carried out using a jet facility at the Hypersonic High-enthalpy Wind Tunnel at Kashiwa Campus of the University of Tokyo. The unheated, Mach 1.8 jet was ideally expanded through a 20-mm diameter converging-diverging nozzle. Although the facility is not anechoic, nearby reflecting surfaces were wrapped in fiberglass. Favorable matches to anechoic measurements by Greska [22] were shown previously by Akamine *et al.* [23]

#### 3.2 Microphone Arrays

Data from two microphone arrays are shown in this paper. First, G.R.A.S. 40BE Type 1 prepolarized microphones were used to create a 16-channel polar microphone arc with  $5^\circ$  resolution spanning  $15 - 90^\circ$ , with angles measured relative to the jet exhaust centerline. The microphones were located at a radial distance of 40 nozzle diameters ( $D_j$ ) and centered  $10 D_j$  downstream from the jet exit. The near-field array consisted of four two-dimensional intensity probes comprised of G.R.A.S. 46BG microphones, which have sensitivities less than 0.3 mV/Pa and permit peak sound pressure level measurements in excess of 180 dB. The microphones were arranged in an equilateral triangle by 3D-printed holders, with a microphone at the center of the triangle such that the distance between the center and the vertices was 25.4 mm. The arrays are shown in Fig. 1. For all measurements, the microphone gridcaps were removed.

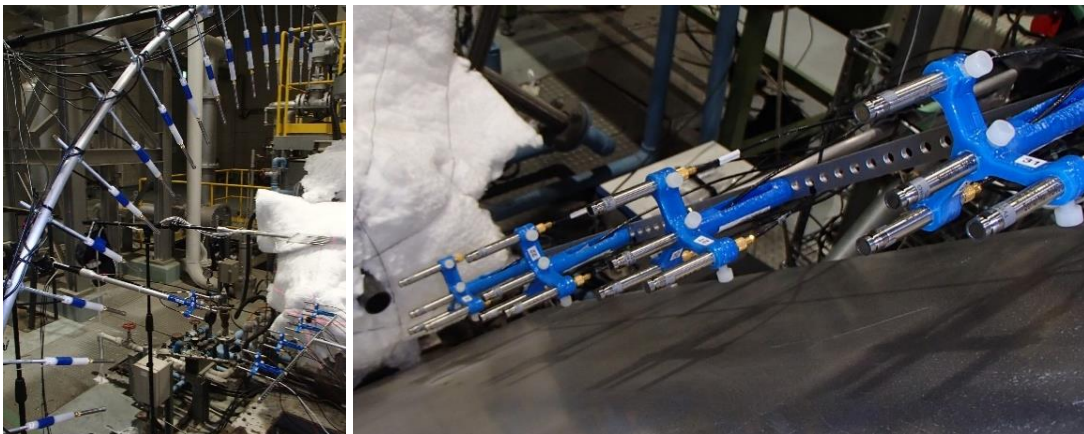


Figure 1. Left: Polar microphone array. Right: Near-field vector intensity probe array that was attached to a two-axis positioning system.

#### 3.3 Data Acquisition

Calibrated acoustic pressure waveform data were synchronously acquired at each array position at 204.8 kHz using National Instruments PXI-4498 cards. During each jet blow, which lasted between 60-90 seconds, data were acquired for 6.1 seconds and the near-field microphone array was moved to several positions using a two-axis, stepper-controlled positioning system. For each test, the jet facility ambient pressure, temperature, and humidity were recorded using a Kestrel 4500B weather station.

### 3.4 Level-based results

Some level-based results are instructive in demonstrating the need for the PAGE method in determining the vector intensity for this laboratory-scale jet. The power spectral density (PSD) and overall sound pressure level (OASPL) at the 40 diameter ( $D_j$ ) polar arc are shown in Fig. 2. First, the OASPL is a maximum between  $30 - 35^\circ$  relative to the jet exhaust centerline, which is characteristic of a Mach 1.8 unheated jet. Second, the PSD peak frequency shifts between 2 kHz at  $15^\circ$  to 5-6 kHz at  $65^\circ$ , beyond which the peak remains relatively constant. Given the relatively high peak frequency, one of the key points of Fig. 2 is the significant limitation of the traditional cross-spectral calculation method to obtain a broadband aeroacoustic source characterization with the intensity probe geometry. Calculation bias errors limit the vector intensity field to relatively low frequencies, as prior laboratory analysis [24] of this probe configuration suggests magnitude errors exceed 1 dB at 2.5 – 3 kHz and directional errors begin to grow rapidly at approximately 5 kHz. Thus, the broadband vector acoustic field must be obtained using an alternate processing method.

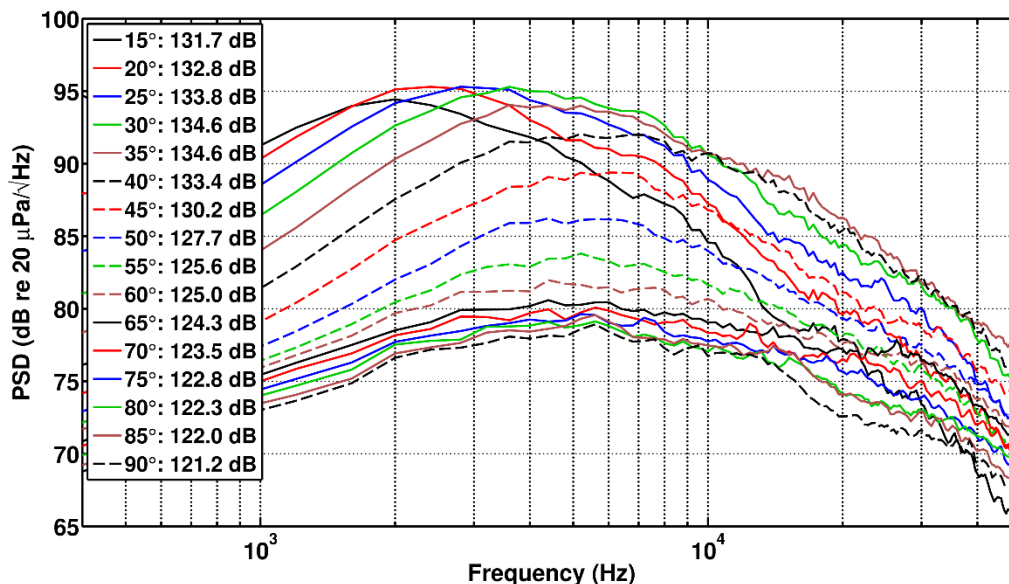


Figure 2. Power spectral densities and overall sound pressure levels (in the legend) at the microphone arc located at a radial distance of  $40 D_j$  and centered  $10 D_j$  downstream of the nozzle exit.

## 4 INTENSITY ANALYSIS

In this section, a progression of analyses that demonstrate the utility of the PAGE method is shown. First, vector and level-based maps from the traditional cross-spectral intensity method are shown. The results become nonphysical above a certain frequency. Second, the ability to phase-unwrap the transfer functions between probe microphones is demonstrated. Third, a comparison the traditional and PAGE methods at a few specific frequencies is shown. Finally, maps and a source characterization based on PAGE-calculated intensities are presented.

### 4.1 Traditional Cross-Spectral Method

Figure 3 displays narrowband (50-Hz resolution) intensity vector and level-based maps calculated using the traditional cross-spectral method for six octave band center frequencies,

1000 Hz to 32000 Hz. These frequencies correspond to a jet Strouhal number range of 0.042 to 1.34, which is sufficient to characterize the low, peak, and high-frequency radiation from the jet. In Fig. 3, the jet shear layer is denoted by the dashed line, and vectors appear at all measurement locations. For ease in viewing the vector field, the vector lengths have been scaled by the sixth root of the intensity magnitude. In the intensity level map, color gradations represent 1 dB changes in level. To help provide physical level approximations in the regions where there are not vector measurements, the sound pressure levels at  $40 D_j$  (virtually equal to the intensity levels) are included in the calculation of the interpolated levels. More detailed examination of the frequency-dependent characteristics are discussed in the context of the PAGE method, but the traditional intensity calculations clearly yield nonphysical results for 8 kHz and above.

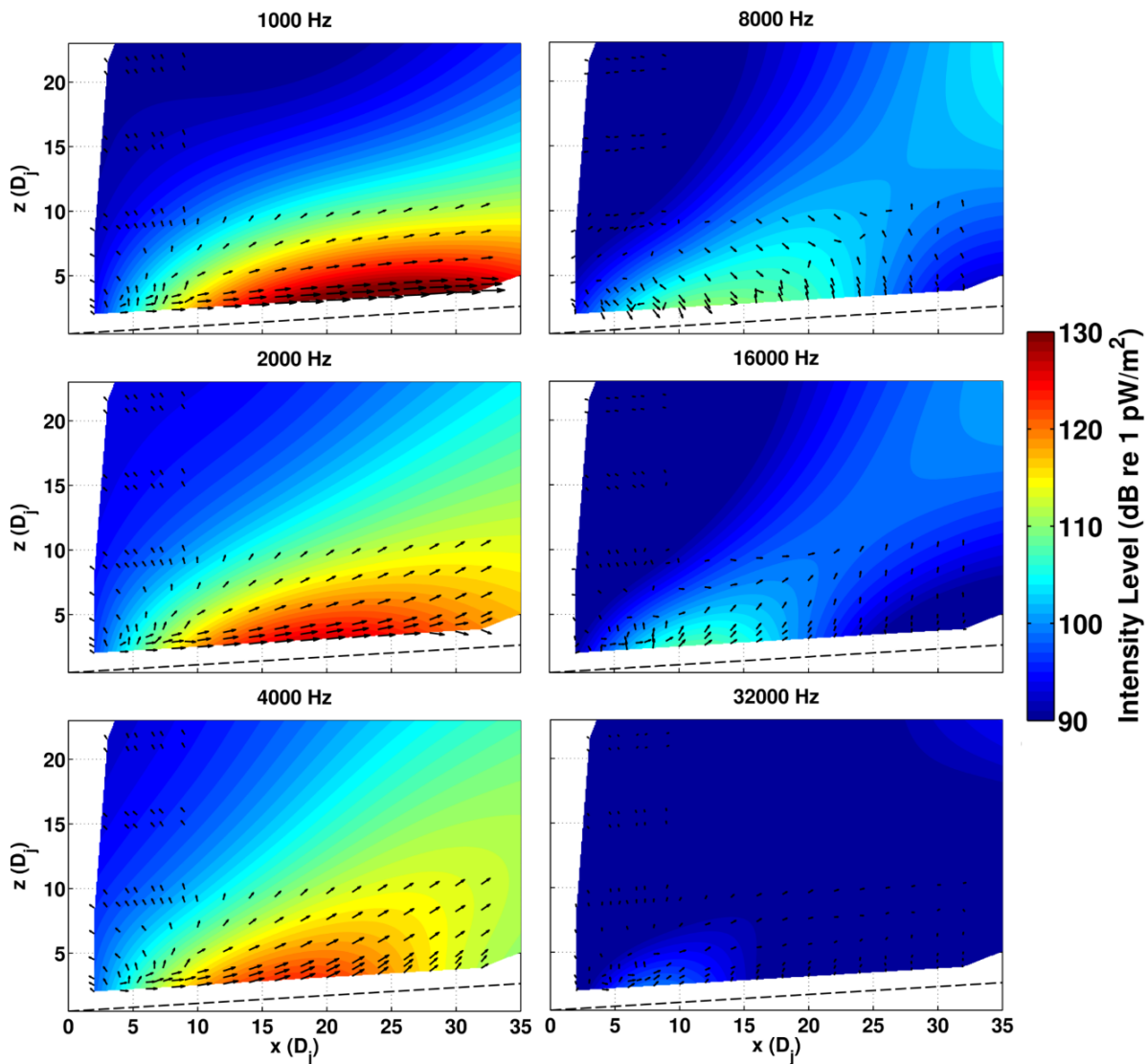


Figure 3. Traditional calculation of intensity vectors at six octave band center frequencies for a Mach 1.8 uheated jet.

## 4.2 PAGE Phase Unwrapping

As described in Sec. 2, the PAGE method formulation allows for the possibility to unwrap the phase of the transfer function and increase the intensity calculation bandwidth. Bandwidth extension is impossible with the traditional method because it works directly with weighted sums of complex cross spectra, which cause significant bias errors as the spatial Nyquist frequency is approached. [13] Figure 4 shows two representative examples of the phase of the transfer function between microphones on intensity probes located at different points in the jet field. In each plot, there are six curves, representing the wrapped and unwrapped frequency-dependent phase for the three outer microphones relative to the center microphone. The results show clearly why, for the sound field radiated by a jet plume, the PAGE method is a viable alternative to the decades-old method of calculating intensity from the complex cross spectra of multimicrophone probes. At the left of Fig. 4, the unwrapping occurs between one and three times for the three transfer functions considered, and the unwrapped phase continues smoothly out to 40 kHz. On the right, unwrapping occurs between zero and three times for the three functions, and irregular jumps occur beyond 35 kHz. The jumps may be due to scattering from the microphones or probe holder or reflections in the non-anechoic environment and merit further investigations. In analyzing the transfer function phase at various probe locations, these irregular jumps occasionally occur at lower frequencies, in the 15-20 kHz range, but in many other cases, the transfer function phase unwrapping continues smoothly to 40 or 50 kHz. Thus, because the PAGE intensity calculation in Eq. (4) involves simply a scaled mean-square pressure calculation multiplied by the phase gradient, phase unwrapping is a powerful method for extending probe bandwidth well beyond traditional limits for broadband sources.

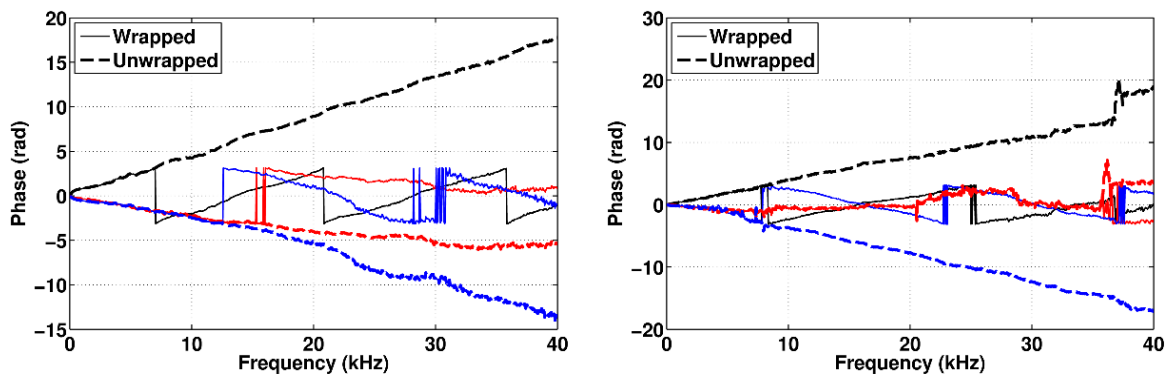


Figure 4. Transfer function phase unwrapping for the outer three probe microphones relative to the probe center microphone for two intensity probes at different locations in the jet noise field.

## 4.3 Traditional Method versus PAGE Method

Displayed in Fig. 5 are comparisons between sound pressure level and sound intensity level calculated according to both the traditional and PAGE methods. The comparison is done for three frequencies: 2 kHz, where from prior laboratory experiments [24] good agreement is expected between the intensity calculation methods, 4 kHz, where minor differences in intensity angle, but an appreciably lower amplitude for the traditional method are expected, and 8 kHz, by which point the traditional method has broken down, with vectors pointing in entirely erroneous directions. These expectations are confirmed in Fig. 5. At 2 kHz, there are differences in the calculation methods intensity vectors closest to the shear layer at the beginning and end of the high-amplitude regions, but the fields are otherwise extremely consistent. At 4 kHz, the

traditional method has vectors, particularly those near the shear layer, that are shallower and with amplitudes that are about 5 dB lower than the PAGE method. At 8 kHz, the traditional method yields vectors that point toward the source in many cases, without a well-defined energy flow.

The comparison between the PAGE intensity and sound pressure level maps provides a benchmark for the PAGE method. The complex intensity is the sum of the active and reactive intensities, with the active intensity obtained from the portion of the particle velocity that is in phase with the acoustic pressure [see Eqs. (3) and (4)]. For propagating wave fields, i.e. planar, cylindrical, or spherical wave fields, this results in  $|I| \propto \overline{P^2}$  and near equivalence of the sound pressure and intensity levels. For these frequencies, the PAGE intensity levels closely approximate the sound pressure levels, to within 1 dB, at most locations. At low frequencies (less than 2 kHz) and close to the shear layer, there are some differences between the pressure and intensity levels, presumably because the microphones are located within the hydrodynamic pressure field. Location of intensity probes within the hydrodynamic near field is further considered as part of the PAGE near-field intensity characterization in Sec. 4.4.

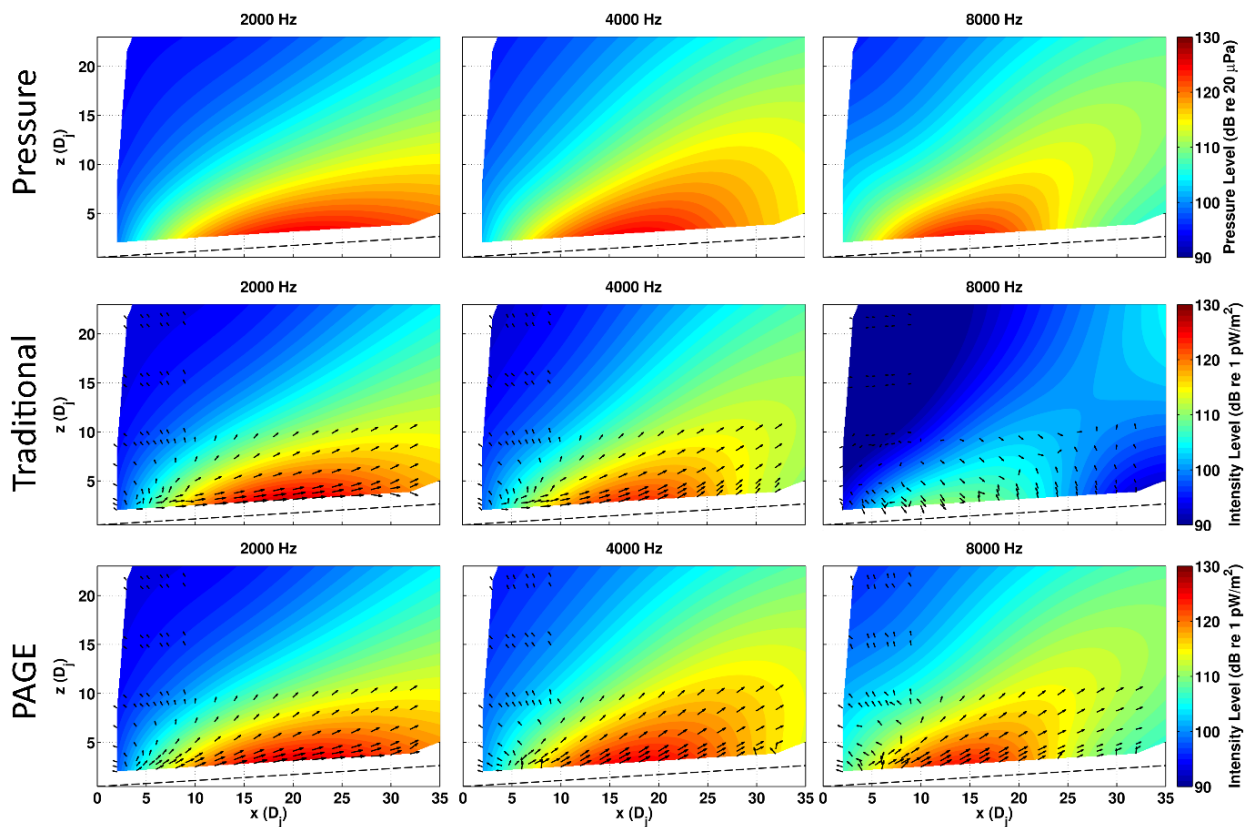


Figure 5. Near-field maps for 2000, 4000, and 8000 Hz based of the sound pressure level and the acoustic vector intensity obtained with the traditional calculation and the PAGE method.

#### 4.4 PAGE Method Near-field Intensity Characterization

The success of the phase unwrapping method and concordance of intensity and sound pressure levels suggest that the PAGE method, which has been previously used with various probe geometries to produce full-scale rocket and military jet noise source characterizations from as low as 30 Hz to as high as 6 kHz, can be extended to much higher frequencies for this

experiment. While less important for a full-scale rocket motor with dominant radiated intensity below 100 Hz [8,10], the frequencies in the several kilohertz range are critical to the characterization of this small-scale jet. Figure 6 displays narrowband intensity vector and level-based maps for six octave-band frequencies from 1000 Hz to 32000 Hz, the same frequencies as Fig. 4. The same sixth-root amplitude scaling used in Figs. 4 and 5 is applied. The results in Fig. 6 show the ability of the PAGE method to characterize the broadband acoustic energy flow from a laboratory-scale jet, whereas the traditional method is severely bandlimited. Analysis is on-going and is being complemented by high-speed Schlieren imaging [25], but trends appear physical over the entire frequency range. First, the angle of the principal radiation lobe increases with frequency, while the sideline radiation appears to be relatively consistent. Second, the source region that produces this lobe significantly contracts and shifts upstream for much of the frequency range. However, before discussing this statement more quantitatively, some additional comments regarding Fig. 6 are merited.

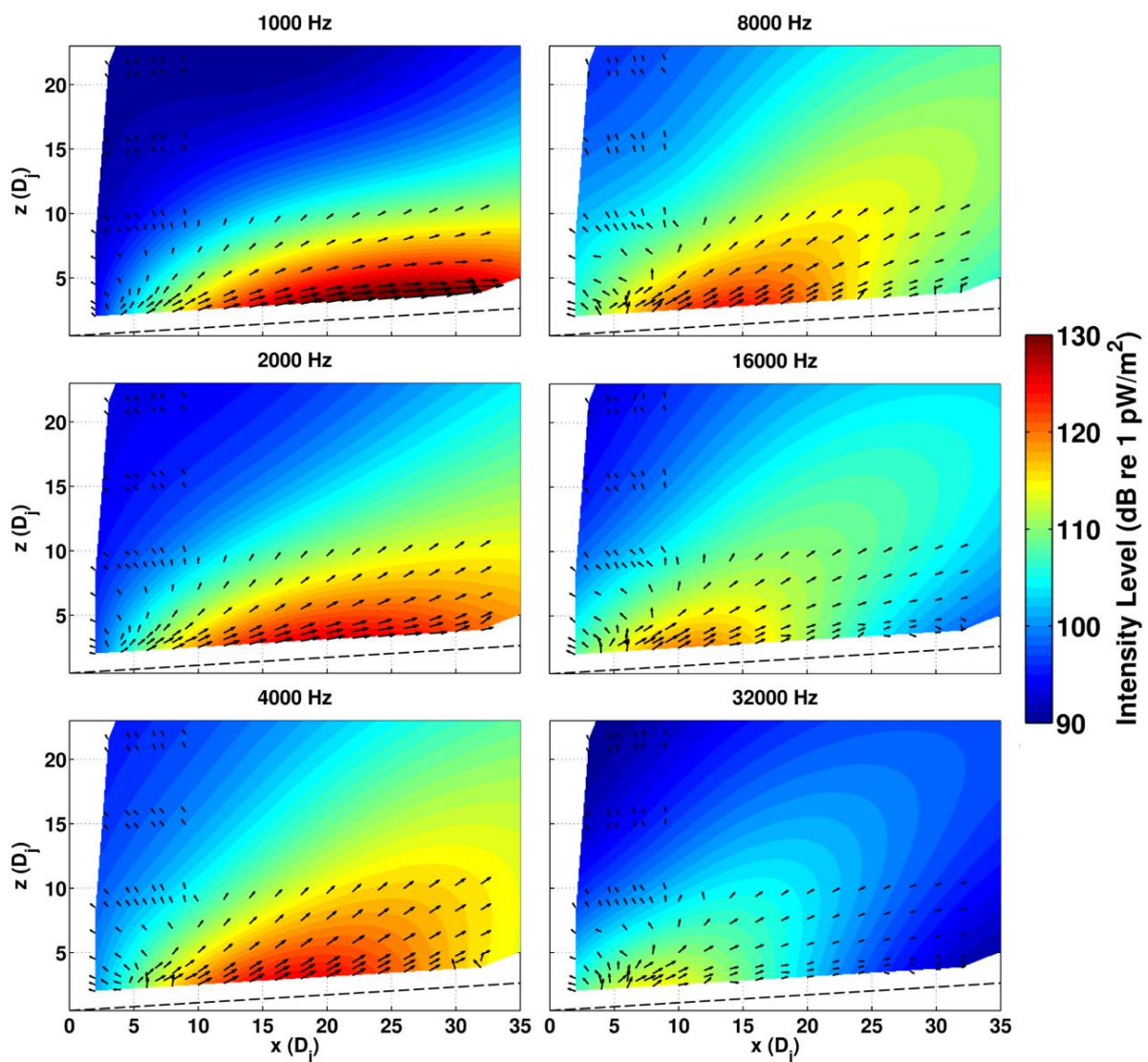


Figure 6. PAGE-calculated intensity vectors at four frequencies for a Mach 1.8, unheated jet.

Additional features in Fig. 6 are noteworthy, although more in-depth analysis will largely be saved for further investigations. First, at 1 kHz and to some extent, 2 kHz, the intensity probe locations closest to the jet can be described as being in the hydrodynamic field because the vectors are directly parallel to the jet shear layer. This phenomenon was also evident in Fig. 4, with the traditional processing method, i.e., it is not an artefact of the PAGE processing method. At 1 kHz (Strouhal number of 0.042), these closest vectors dominate the intensity level and demonstrate the propagation behavior of the low-frequency spectral increases in pressure traditionally associated with the hydrodynamic field. At 2 kHz, the vectors closest to the shear layer are again parallel to the jet boundary downstream of approximately  $20 D_j$ . Additional study of this phenomenon is required, because although the directionality of these components, obtained through the transfer function phase gradient, is clear, the effect of the hydrodynamic phase speed on the calculation of intensity levels is in question. At 4 and 8 kHz, which serve to characterize the peak-frequency region of the spectra around the maximum radiation direction, the directionality of the intensity vectors point to an extended Mach wave source region, with a significant contraction of length in source region between the two frequencies. Furthermore, at these frequencies, there is a rapid change in radiation characteristics between the downstream Mach wave radiation and the sideline radiation. At 16 kHz and 32 kHz, there is a less well-defined transition between the radiation in these two directions; furthermore, the sideline radiation becomes relatively greater in amplitude. Based on the physical consistency of the vector magnitudes and directions, which are well correlated with the  $40 D_j$  frequency-dependent pressure levels, the PAGE method extends the upper useable frequency of the multimicrophone probe hardware to beyond 30 kHz, approximately 10 times the traditional limit.

These intensity measurements have the potential to lend physical insight to source characteristics beyond prior far-field phased arrays studies that have attempted to identify noise source distributions as a function of angle (e.g., see Ref. [26] for a Mach 1.9 jet). As an initial attempt at quantifying the apparent source region as a function of frequency, the line of intensity vectors for probe locations spanning  $z = 6.5$  to  $8.4 D_j$  are used to ray-trace back to the jet centerline. Linear interpolation between measurement points is used to determine the location of points at which the sound intensity level is within 3-dB down of the maximum SIL along the measurement line and the intensity vectors within this region are traced back to the jet centerline. The farthest upstream and downstream intercepts of the ray-traced vectors along the centerline are used to define the maximum source region. The results of this approach, which has been used in prior military jet and rocket noise investigations [10-12], are shown in Fig. 7 from 1 and 32 kHz. From 3 - 23 kHz, the source region contracts from  $x = 8.5 - 15.3 D_j$  to  $1.8 - 2.9 D_j$ . The behavior below 3 kHz and above 23 kHz is tied to the low and high-frequency phenomena already mentioned – the hydrodynamic field influence and the blurring between the sideline and downstream radiation phenomena. Below 3 kHz, the vector angles shift toward the shear layer as the offset in  $z$  is decreased. This causes the ray-traced source region to shift far upstream to clearly nonphysical locations. At frequencies greater than 23 kHz, the blending of the downstream and sideline radiation produces a 3-dB region that, when ray-traced, broadens. The upstream radiation is now within the 3-dB down region and accounts for the suddenly larger downstream centerline intercept, while the downstream radiation results in the smoothly varying upstream extent of the source. It is important to note that other source localization criteria or methodologies are possible, and far-field localization techniques will likely result in different source interpretations. This approach yields the dominant source

location for a Strouhal number range of 0.13 to 0.97, with additional physical insights regarding the source characteristics above and below that frequency range.

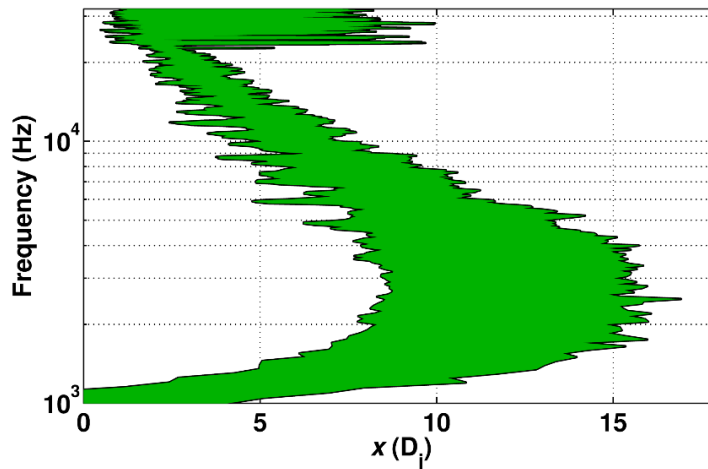


Figure 7. Apparent source region extent at the Mach 1.8 unheated jet centerline as a function of frequency as ray-traced from the probe locations within 3 dB of the maximum intensity level between  $z = 6.5$  and  $8.4 D_j$ .

## 5 CONCLUSIONS

In this paper, a new method for the calculation of vector acoustic intensity from multiple pressure microphone measurements has been applied to the aeroacoustic source characterization of a supersonic, laboratory-scale jet. Although additional research is required to fully validate source characteristics, the bandwidth of traditional intensity measurements for the same probe hardware has been increased by approximately 10 times. Because prior measurements of full-scale rocket and military jet noise environments had suggested an upper frequency improvement of approximately three to five times, this finding is significant. To verify these results with a broadband, deterministic sound field, a complementary anechoic laboratory experiment is planned. This experiment and analytical studies will further establish the PAGE method performance characteristics and may influence measurement standards. Regarding this specific application to a supersonic jet, additional aeroacoustics analyses will provide insight into the frequency-dependent characteristics of jet noise radiation, including the nature of the hydrodynamic field and the sharp transition between the downstream, Mach wave, and sideline radiation.

## ACKNOWLEDGMENTS

The measurements were supported under a travel invitation fellowship by the Japan Society for the Promotion of Science. Analysis was supported in part through a National Science Foundation grant to study the PAGE method and its applications.

## REFERENCES

- [1] ISO 9614-1:1993, Acoustics—Determination of sound power levels of noise sources using sound intensity—Part 1: Measurement at discrete points (International Organization for Standardization, Geneva, Switzerland, 1993).

- [2] ISO 9614-2:1996, Acoustics—Determination of sound power levels of noise sources using sound intensity—Part 2: Measurement by scanning (International Organization for Standardization, Geneva, Switzerland, 1996).
- [3] ISO 9614-3:2002, Acoustics—Determination of sound power levels of noise sources using sound intensity—Part 3: Precision method for measurement by scanning (International Organization for Standardization, Geneva, Switzerland, 2002).
- [4] T. Astrup, “Measurement of sound power using the acoustic intensity method –A consultant’s viewpoint,” *Appl. Acoust.* 50, 111–123 (1997)
- [5] ISO 15186-2:2010, Acoustics—Measurement of sound insulation in buildings and of building elements using sound intensity—Part 1I: Field measurements (International Organization for Standardization, Geneva, Switzerland, 2003).
- [6] S. M. Jaeger and C. S. Allen, “Two-dimensional sound intensity analysis of jet noise,” *AIAA Paper 93-4342* (1993).
- [7] S. R. Ventakesh, D. R. Poak, and S. Narayana, “Beamforming algorithm for distributed source localization and its application to jet noise,” *AIAA J.* 41, 1238–1246 (2003).
- [8] K. L. Gee, J. H. Giraud, J. D. Blotter, and S. D. Sommerfeldt, “Energy-based acoustical measurements of rocket noise,” *AIAA Paper 2009-3165* (2009).
- [9] K. L. Gee, J. H. Giraud, J. D. Blotter, and S. D. Sommerfeldt, “Near-field acoustic intensity measurements of a small solid rocket motor,” *J. Acoust. Soc. Am.* 128, EL69-EL74 (2010).
- [10] K. L. Gee, E. B. Whiting, T. B. Neilsen, M. M. James, and A. R. Salton, “Development of a near-field intensity measurement capability for static rocket firings,” *Proc. 30<sup>th</sup> Int. Symp. Space Tech. Science*, Kobe, Japan, July 2015.
- [11] T. A. Stout, K. L. Gee, T. B. Neilsen, and A. T. Wall, “Acoustic intensity near a high-powered military jet aircraft,” *J. Acoust. Soc. Am.* 138 EL1-EL7 (2015).
- [12] T. A. Stout, K. L. Gee, T. B. Neilsen, A. T. Wall, and M. M. James, “Source characterization of full-scale jet noise using vector intensity,” *Noise Control Eng. J.* 63, 522-536 (2015).
- [13] D. C. Thomas, B.Y. Christensen, and K. L. Gee, “Phase and Amplitude Gradient Method for the Estimation of Acoustic Vector Quantities,” *J. Acoust. Soc. Am.* 137, 3366-3376 (2015).
- [14] F. J. Fahy, “Measurement of acoustic intensity using the cross-spectral density of two microphone signals,” *J. Acoust. Soc. Am.* 62, 1057-1059 (1977).
- [15] G. Pavic, “Measurement of sound intensity,” *J. Sound Vib.* 51, 533–545 (1977).
- [16] J.-C. Pascal and J.-F. Li, “A systematic method to obtain 3D finite-difference formulations for acoustic intensity and other energy quantities,” *J. Sound Vib.* 310, 1093 – 1111 (2008).
- [17] C. P. Wiederhold, K. L. Gee, J. D. Blotter, and S. D. Sommerfeldt, “Comparison of methods for processing acoustic intensity from orthogonal multimicrophone probes,” *J. Acoust. Soc. Am.* 131, 2841-2852 (2012).
- [18] C. P. Wiederhold, K. L. Gee, J. D. Blotter, S. D. Sommerfeldt, and J. H. Giraud, “Comparison of multimicrophone probe design and processing methods in measuring acoustic intensity,” *J. Acoust. Soc. Am.* 135, 2797-2807 (2014).

- [19] J. A. Mann III, J. Tichy, and A. J. Romano, “Instantaneous and time-averaged energy transfer in acoustic fields,” *J. Acoust. Soc. Am.* 82, 17–30 (1987).
- [20] J. A. Mann III and J. Tichy, “Acoustic intensity analysis: Distinguishing energy propagation and wave-front propagation,” *J. Acoust. Soc. Am.* 90, 20–25 (1991).
- [21] J. A. Mann III and J. Tichy, “Near-field identification of vibration sources, resonant cavities, and diffraction using acoustic intensity measurements,” *J. Acoust. Soc. Am.* 90, 720–729 (1991).
- [22] B. Greska, “Supersonic jet noise and its reduction using microjet injection,” Ph.D. thesis, The Florida State University, FAMU-FSU College of Engineering, 2005.
- [23] M. Akamine, Y. Nakanishi, K. Okamoto, S. Teramoto, T. Okunuki, and S. Tsutsumi, “Acoustic phenomena from correctly expanded supersonic jet impinging on inclined plate,” *AIAA J.* 53, 2061-2067 (2015).
- [24] D. K. Torrie, E. B. Whiting, K. L. Gee, and T. B. Neilsen, “Initial laboratory experiments to validate a phase and gradient estimator method for the calculation of acoustic intensity,” *J. Acoust. Soc. Am.* 137, 2402 (2015).
- [25] M. Akamine, K. Okamoto, K. L. Gee, T. B. Neilsen, S. Teramoto, S. Tsutsumi, T. Okunuki, “Comparison of acoustic intensity vectors with SPL and phase distributions of supersonic jet,” 8<sup>th</sup> Asian Joint Conference on Propulsion and Power, Mar. 2016.
- [26] C. K. W. Tam, K. Viswanathan, K. K. Ahuja, and J. Panda, “The sources of jet noise: Experimental evidence,” *J. Fluid Mech.* 615, 253-292 (2008).